Article:
Palacios, A, Bradley, D, Wang, Q et al. (2021) Air/Fuel Mixing in Jet Flames. Proceedings of the Combustion Institute, 38 (2). pp. 2759-2766. ISSN: 1540-7489

https://doi.org/10.1016/j.proci.2020.07.083

Air/Fuel Mixing in Jet Flames

Adriana Palacios[a*], Derek Bradley[b], Qiang Wang[c,d], Xin Li[c], Longhua Hu[c]

[a]*Fundacion Universidad de las Americas, Puebla, Department of Chemical, Food and Environmental Engineering, Puebla 72810, Mexico.*

[b]*University of Leeds, School of Mechanical Engineering, Leeds LS2 9JT, UK.*

[c]*State Key Laboratory of Fire Science, University of Science and Technology of China, Hefei, Anhui 230026, China.*

[d]*School of Automotive and Transportation Engineering, Hefei University of Technology, Hefei, Anhui, 230009, China.*

*Corresponding author email: adriana.palacios@udlap.mx

Colloquium: CC/CCC Submissions.

Total length of the paper: 6198 of 6200 maximum words.

List word equivalent lengths:

Main Text = 3351

References = (27 references + 2) x (2.3 lines/reference) x (7.6 words/line) = 507

Figure 1 = (65 mm + 10 mm) x (2.2 words/mm) x (2) + (22) = 352

Figure 2 = (118 mm + 10 mm) x (2.2 words/mm) x (2) + (16) = 580

Figure 3 = (53 mm + 10 mm) x (2.2 words/mm) x (2) + (29) = 307

Figure 4 = (60 mm + 10 mm) x (2.2 words/mm) x (2) + (32) = 340

Figure 5 = (48 mm + 10 mm) x (2.2 words/mm) x (2) + (23) = 279

Figure 6 = (70 mm + 10 mm) x (2.2 words/mm) x (2) + (7) = 359

Equation 1 = (1 eqn line + 2 blank lines) x (7.6 words/line) x (1) = 23

Equation 2 = (2 eqn line + 2 blank lines) x (7.6 words/line) x (1) = 31

Equation 3 = (1 eqn line + 2 blank lines) x (7.6 words/line) x (1) = 23

Equation 4 = (1 eqn line + 2 blank lines) x (7.6 words/line) x (1) = 23

Equation 5 = (1 eqn line + 2 blank lines) x (7.6 words/line) x (1) = 23

Abstract

The paper examines eight diverse regimes in which fuels can mix and react with air. These comprise: (i) Lifted subsonic; and (ii) supersonic jet flames, with (iii) and without (iv) cross flows; (v) Rim-attached flames; (vi) Early Downwash flames; (vii) Downwash-attached jet flames; and (viii) Fire Whirls.

Correlations of characteristics within these regimes are principally in terms of a dimensionless Flow Number, U^*, Cross Flow Reynolds number, Re_c, and, for Fire Whirls, a dimensionless Critical Velocity, CV. Boundaries of seven of the eight regimes are identified, through plots of U^*, against Re_c, and of the eighth through a plot of CV against U^*. The circumstances of transitions between regimes are identified. The study involves a variety of CH_4 cross flow flame measurements, in a wind tunnel. Cross flows can initially create a small lee-side flame downwash, due to the depression in pressure. With increasing fuel flow this might extend 1.3 m downwards from the horizontal tip of the vertical burner. Jet flames can attach to the downwash, which can become significant above $Re_c \approx 2{,}000$. More extensive downwash might further delay blow-off. Regime boundaries are constructed on the U^*/Re_c diagram covering lifted flames, early downwash, and downwash-attached flames. The most powerful flames tend to be lifted, choked, flames, with cross flow, and fire whirls. Combustion becomes less efficient at high Re_c and low U^*, although CH_4 was efficiently reacted.

Experimental values of the ratio of fuel to air velocity, u/u_c, of CH_4 flames ranged between about 10 and 30 for lifted flames, and between 0.3 and 3.6, at blow-off, for rim-attached flames. The latter comprise an important category, often intermediate between lifted flames and downwash-attached flames.

Keywords: Cross flow; downwash; burner-attached flames; rim-attached flames; fire whirls.

1. Introduction

The paper considers the different ways in which a jet of fuel and air can interact. The fundamental interaction of a fuel jet, entraining surrounding atmospheric air, makes *lifted jet flames* a good starting point [1-5]. Usually the jet is *subsonic*, but it can become *choked*, creating shock waves. Such jet flames are characterised in terms of a dimensionless jet flow number, U^*, suggested by computational studies and experiments [1,2]:

$$U^* = \left(u/S_L\right)\left(\delta/D\right)^{0.4}\left(P_i/P_a\right), \tag{1}$$

where u is the mean fuel jet velocity at the pipe exit plane, S_L, the maximum laminar burning velocity, D the fuel pipe internal diameter, δ, the flame thickness, given by ν/S_L, and P_i/P_a the ratio of upstream stagnation to atmospheric pressure.

The role of the normalised pipe diameter, D/δ, is crucial. If it is small, entrained air might quench the flame, leading to blow-off. Computations show the mixture at the leading edge of the flame to be close to that at which the laminar burning velocity has its maximum value [1].

Another mixing procedure involves a *cross flow* of air, perpendicular to the faster moving fuel jet [3,6,7]. As u_c increases, it deflects mainly the upper part of the flame, with little effect on its most reactive leading edge, at the lift-off distance, L, measured from the pipe exit plane to the flame tip. As u_c exceeds u, L eventually begins to decrease and the flame attaches to the pipe rim at the leeward side, creating a *rim-attached* flame [8]. The increase in u_c makes the flame more horizontal, prior to blow-off.

At a lower fuel velocity, as u_c increases, the depression in pressure on the pipe leeward side, increases a downwash flow velocity. A small flame is created at the leeward rim, and as u_c and u further increase, an early *downwash flame* [6,8,9] develops that becomes *fully developed*.

The fuel flow can then be increased to maintain a growing *downwash-supported jet flame* [8,10]. The paper identifies maximum fuel flow rates, through U^*, that can be sustained by the downwash, through Re_c. Here the Reynolds number, $Re_c = u_c D_o/\nu_a$, with D_o the pipe external

diameter, and ν_a the kinematic viscosity of the cross flow air. Combustion becomes increasingly inefficient at high Re_c and low U^*, although CH_4 is efficiently reacted.

Another fuel/air interaction is created by sideways tangential air circulation around, and into, a central large fuel flow, not necessarily with a high velocity, with the generation of a *fire whirl* at a critical, not so high, wind velocity. In a laboratory this can be achieved by tangential air flow vertically around a central pool of evaporating fuel on a central disk, that might be rotated [11,12]. With increasing rotation the fuel/air flow tends to laminarise in the lower plume, with recirculation enhancing air entrainment.

The rotating chimney thus formed creates a high velocity, with low ground pressure. Large scale atmospheric fire whirls, at velocities exceeding the Critical Velocity [13], within wild fires, are more erratic than laboratory whirls [14]. Different flames are discussed in the light of new experimental data.

2. Lifted flames, cross flows, and downwash

2.1 Basic considerations

As fuel flow rates in jet flames increase, eventually a point is reached at which further entrainment becomes excessive, the flame extinguishes, and blows-off from the burner. Initially, it is possible for the lifted fuel jet to sustain also an increasing cross flow of air. Fuel/air mixing is enhanced by the air/fuel vortex within the lift-off zone, between the pipe exit plane and flame leading edge [15,16]. Downstream of this leading edge, the atmosphere becomes the only source of air in this analytical approach. However, an increasing cross flow of air cannot be sustained, and eventually, to maintain reaction, the fuel flow rate has to be decreased, followed by a decrease in the air flow rate. At the initial higher values of U^*, u/u_c is about 20. With the decreasing reaction rates, this ratio falls to about 10. The flames might no longer be lifted, and downwash might develop on the leeward side.

It is fruitful to define the ratio of air to fuel moles, C, by:

$$C = (\rho_a u_c DL/M_a)/(\rho_j u \pi D^2/4M_j) = \left(\frac{L}{D}\right)\left(\frac{4M_j\rho_a}{\pi M_a \rho_j}\right)\left(\frac{u_c}{u}\right), \quad (2)$$

where M_a is the molecular mass of air, M_j the molecular mass of fuel, ρ_a the density of the air, and ρ_j that of jet fuel at the pipe exit plane.

Evaluation of L/D was aided by measurements in the wind tunnel of the State Key Laboratory of Fire Science (SKLFS) [7]. With atmospheric propane-lifted jet flames, u_c decreased to about u/u_c=10. As u_c was increased the shape of the lower part of the flame did not change much, while the upper part bent over, becoming nearly parallel to the cross flow. It is to be anticipated that L/D would depend upon f, the ratio of fuel to air moles for maximum burning rate. Values of f are 0.046 for C_3H_8, 0.107 for CH_4 and 0.756 for H_2.

The value of L/D remained consistent, until just prior to blow-off, with:

$(L/D)f = 0.0002U^{*2} + 0.086\ U^* - 0.174$, for propane, and (3)

$(L/D)f = 0.15U^* - 0.2$, for methane. (4)

Prior to blow-off, the value was 0.8 of that given by these expressions.

2.2 Lifted flame-cross flow characteristics

Figure 1 shows the C_3H_8/air experimental cross flow, subsonic, blow-off data of Kalghatgi [6] at atmospheric pressure, when processed in this way, with U^*, at blow-off, U_b^*, as a function of C. The dependency of blow-off upon pipe diameter also is shown by data for the three highest pipe diameters, normalised by the laminar flame thickness, δ_k. This is defined by the location of a temperature T^o, below which there is no reaction [17], evaluated from:

$$\delta_k = \left(k/C_p\right)_{T^o}/(\rho_u S_L), \quad (5)$$

where C_p is specific heat at constant pressure, ρ_u unburned gas density, and k the thermal conductivity, with values of T^o from [17]. Stable flames exist within the separate peninsulas for values of D/δ_k equal to, or greater than, the given values.

The lower of the two broken curves is derived from the atmospheric propane data in [7], with the exceptionally low values of D/δ_k = 16 for a Tibetan atmospheric pressure of 64 kPa, arising from the increased δ_k at low density.

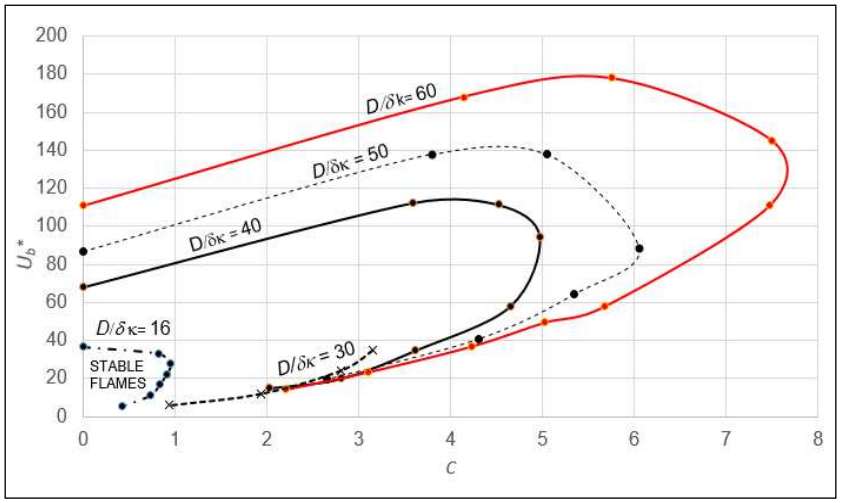

Fig. 1. Blow-off limits of stable propane lifted flames with air cross flows, in terms of U_b* versus C, for different D/δ_k.

At atmospheric pressure, S_L and δ_k = 0.43 m/s and 0.100452 mm, at 0.64 MPa, and S_L = 0.46 m/s [18]. Pressure dependency laws are in [19]. The importance of higher values of D/δ_k to extend the range of stable flames and U_b* at blow-off, is apparent. As pipe diameters decrease, the increased mixing of fuel with air induces more rapid leaning-off of the mixture, and flame extinction.

Initially, as C increases, so also can burning rate and U_b*. Eventually, the air dilution becomes excessive, reaction rates decline, and it is impossible to maintain the value of U_b*, without an increase in D/δ_k. Combustion is maintained by curtailing increases in C and U*, more sharply at the lower values of D/δ_k.

Similar cross-flow blow-off characteristics were derived for CH_4, also from [6]. Values of S_L and δ_k were 0.39 m/s [20] and 0.1288 mm [21].

2.3 Practical implications

The ratio of the amount of cross flow air mixed with fuel, C, to that ultimately required for the maximum burning rate mixture is Cf. This additional air is acquired through entrainment of atmospheric air by original cross flow air and the reacting fuel jet. The maximum value of C in Fig. 1 is about 7.6 and, with $f = 0.046$, this implies a proportion of 0.35 of the necessary overall air had been acquired from the directed cross flow. Any further increase would lead to blow-off. For the smallest diameter flame at a much lower U^*, with $C = 1$, the cross flow air proportion was 0.046 of the ultimate requirement. Although such values are approximate, it is of interest that most of the necessary air must come from atmospheric entrainment. However, the flame quenching tendencies induced by cross flows are probably more relevant than those of enhancements. In atmospheric flaring of gases, cross winds can lead to flame extinction, probably significantly more easily for CH_4 and C_3H_8 than H_2 [22].

With stable lifted flames, and values of u/u_c of about 20, as u_c increases and u decreases, the flames become rim-attached. With u_c exceeding u, downwash flames develop on the leeward side [8]. With further increase in u_c jet flames appear, anchored to the downwash turbulent wake flame. Quite strong downwash-attached jet flames can be established. This regime becomes more appropriately expressed in terms of U^* and the cross flow Reynolds number Re_c.

These coordinates are also used as an alternative to the U^*/C coordinates in Fig. 1, for the CH_4 lifted flame with cross flow data from [6]. This new plot appears in Fig. 2, along with additional data, for a total of 6 different values of D/δ_k, with two data sets, at higher D/δ_k, over a limited range.

Also plotted in Fig. 2, at high values of U^* and Re_c, are data for three choked lifted flames, with cross winds and sonic shocks at the pipe exits, that enhance reaction rates [21]. These are shown by the top half-blackened square symbols in Fig. 2. In order of increasing Re_c, the D/δ_k, and fuel mass flow rates are 1,180, 5 kg/s [23], 1,180, 10.7 kg/s [3] and 1,576, 10.7 kg/s,

developing 595 MW [3]. In sharp contrast, the early appearance of downwash is indicated by filled triangles, at $U^* = 0.1$.

3. Jet flame regimes

The present innovative study attempts a new quantitative identification of eight diverse regimes of fuel jet flames in air. Section 2 has introduced many, but my no means all, relevant aspects. Lifted flames in cross flow have been analysed. Rim-attached and downwash flames have been introduced, and feature in what follows, along with downwash-attached flames and fire whirls. All but the fire whirls, which have a separate correlation, are characterised in plots of U^* against Re_c, in the comprehensive Fig. 2. This key figure attempts to identify all the regime boundaries, but some uncertainties remain, and will catalyse further studies.

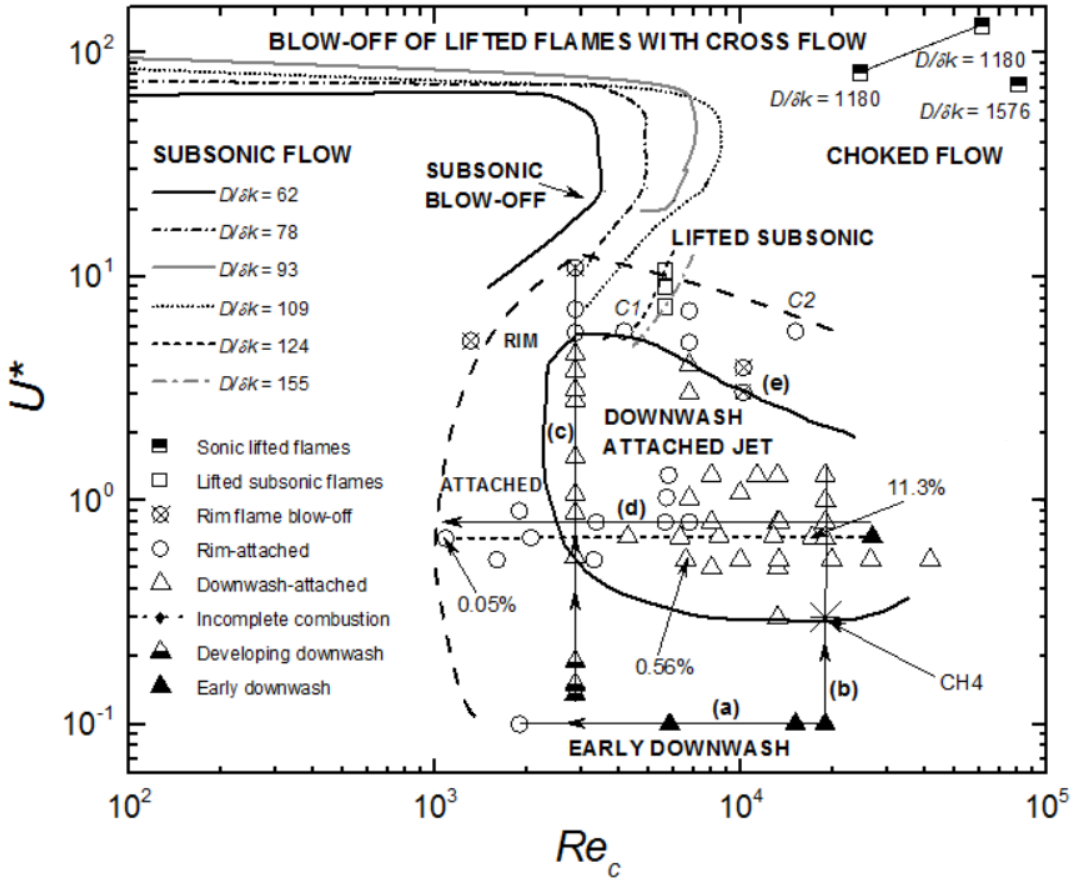

Fig. 2. Different flames regimes, in terms of U^* and Re_c, for subsonic and sonic flows.

4. Generation of downwash flames

This was studied in the SKLFS wind tunnel, with a cross section 1.8 m square and 20 m in length. Air flows, were between 0.5 and 10 m/s, from a 2.7 m diameter impeller, driven by a variable speed 30 kW D.C. motor [7].

Variable flows of propane, with air cross flows, created optimal conditions for the generation of downwash flames, with D = 8, 10, 13 and 15 mm. Air cross flow velocities were measured with a hot-wire anemometer. Shown in Fig. 3(a), is the regime of downwash flames that increases with Re_c and U^*. Values of U^* are relatively low, yet sufficient to maintain an early downwash. A robust flame developed at Re_c = 1,340, U^* = 0.06, with a depth of 21 cm.

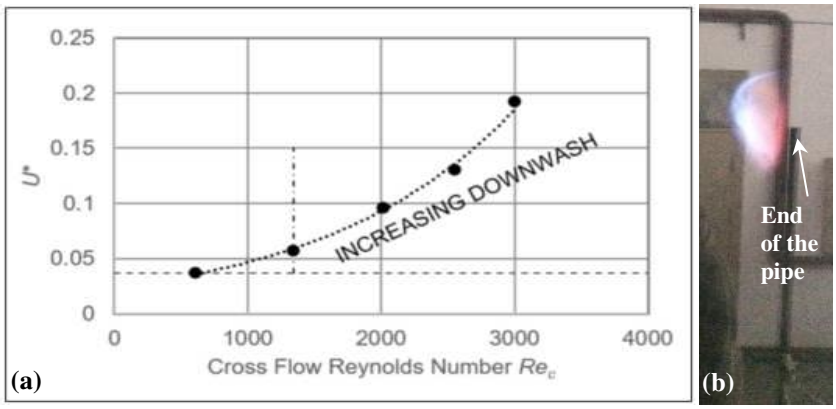

Fig. 3. (a) Developing propane downwash with increasing Re_c and U^*. No downwash below horizontal broken line. (b) Early CH_4 flame downwash, Re_c = 18,860, and U^* = 0.1.

Fig. 3(b) shows a small, early downwash flame at the leeward tip of the fuel pipe. Air flow is from right to left. The flame extends 37 cm downwards, from the top plane of the burner to the bottom of the small vortex downwash flame.

With U^* = 0.1, for values of Re_c between 5,845 and 15,085, flame images were similar, with only limited downwash flows. The combination of high air and low fuel flows prevented any extension of combustion beyond the leeward side at the burner tip, due to the restricted fuel flow.

5. Rim-attached flames

The fuel pipe CH_4 discharge was 80 cm, above the ground. To cover fully the different regimes, five different pipes with internal and external diameters, ranging between 8-28 mm and 10-30 mm, respectively, were employed. The early downwash flame at U^*=0.1, Re_c=18,860 in Fig. 3(b), had excess air, with u=0.54, and u_c=0 m/s. A full downwash flame could only develop through a decrease in u_c and Re_c, or increases in u and U^*.

A decrease in Re_c is considered first, along horizontal line *(a)*, in Fig. 2. With U^*=0.1. It passes through three early downwash triangle symbols at Re_c=18,860, 15,085, and 5,845, with no significant change in the downwash. However, at Re_c=1,886, the flame becomes rim-attached on the leeward side, as shown in Fig. 4(a), with u_c=1 m/s, and u/u_c=0.54. Further reduction in u_c caused flame blow-off.

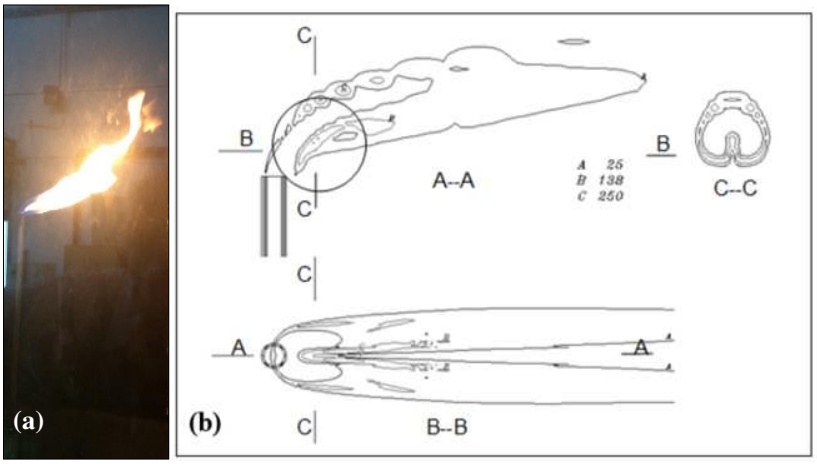

Fig. 4. (a) Flame image at U^* = 0.1, Re_c = 1,886. (b) Computed contours of heat release rate. Rim-attached flame, u = 20 m/s, u_c = 5.5 m/s, U^* = 5.6.

Understanding of the rim-attached CH_4 flame structure was enhanced through numerical simulations of it, using a 3D stretched laminar flamelet RANS code [24]. This enabled higher velocities to be studied than could be obtained experimentally, at higher U^*. Fig. 4(b) shows the computed contours of volumetric heat release rate in MW/m^3, for u=20 m/s, u_c=5.5 m/s, u/u_c=3.6. Inner and outer diameters were 10 and 12 mm, Re_c=4,148. These contours reveal similarities with those of a lifted flame, but are attached to the leeward rim, without lift.

Additional computations, with u_c, also increased to 20 m/s, and Re_c = 15,085, showed a very different, near-horizontal, flame, tenuously attached to the outside rim surface. The two computed points are indicated in Fig. 2 by rim-attached circles, surmounted, respectively, by C1 and C2. These are close to other rim-attached points, aligned with other lifted flames and downwash-attached points. The computed absence of downwash at C2, confirms the experimental evidence, in this same regime of moderately high Re_c and relatively high U^*. Accumulated experimental data suggest rim-attachment requires u/u_c to reach about 0.3, and that blow-off occurs at a ratio of about 3.6. The dashed curve on Fig. 2 indicates the bounds, within which, prior to the generation of downwash-attached jet flames, rim-attachment flames can occur.

6. Downwash-attached jet flames

Again, with the Fig. 3(b) early downwash flame as a starting point, with U^*=0.1, Re_c=18,860, changes are considered for increasing U^*, along the vertical line (*b*) in Fig. 2. Increasing the fuel supply enabled a downwash-attached flame structure to develop. The images in Fig. 5 show the striking increase in the extent of the downwash, to a depth of 1.3 m below the pipe exit plane, for U^*=0.8, 1.0 and 1.3. Starting at U^*=0.1 from the early downwash black triangle in Fig. 2, the subsequent open triangles indicate transitions to a downwash-attached flame. This increasing flame growth is anchored to the upper surface of the downwash. Such flames increased in size with increasing U^*.

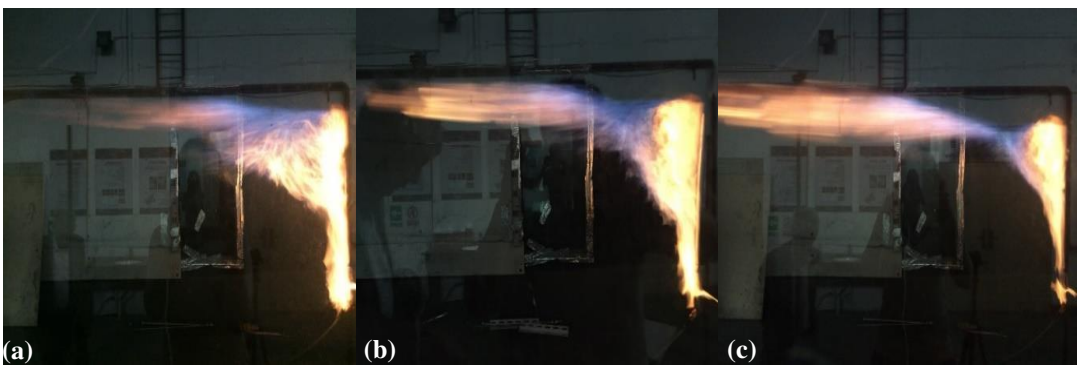

Fig. 5. Downwash-attached methane flames with Re_c = 18,860 and (a) U^* = 0.8; (b) U^* = 1.0; and (c) U^* = 1.3.

Similarly, changes in U^* are now considered along the vertical line (*c*) in Fig. 2, at the lowest Re_c of 2,874. This includes valuable data from [8]. The lowest value of U^* created an early downwash flame that became a downwash-attached flame at U^*= 0.54. The highest downwash-attached value of 4.5 was attained, prior to rim-attachment, at U^*=5.7, and blow-off at U^*=11.0.

In Fig. 2 there are no downwash, downwash-attached, or even rim-attached flames for U^* > 10. This regime is dominated entirely by lifted subsonic and sonic flames, with cross flows extending to high values of Re_c, beyond the Re_c values in Fig. 2. One such operational point, is for a subsonic natural gas lifted flame in cross flow, at Re_c=$1.2 \cdot 10^5$, with D/δ_k=2370, and U^*=14.5 [3].

Finally, changes in Re_c are considered along the horizontal line (*d)*. In Fig. 2, whilst retaining a value of U^* of 0.8, Re_c was reduced by reducing u_c. The initial downwash-attached flame retained its structure until, at Re_c=6,788, it became rim-attached at, u/u_c=1.2, and this persisted down to the lower value of Re_c=1,000. The bold full line, curve (*e*) in Fig. 2, constructs the bounds for the existence of downwash-attached flames. The computed rim-attached points, C1 and C2 are outliers for both these, and other lifted flames. The values of U^* that can be sustained by downwash attachment might be increased by a more extensive volume of downwash.

7. Incomplete combustion

High values of Re_c and low values of U^* are not conducive to the formation of well-mixed flammable mixtures. Johnson and Kostiuk [10,25] have analysed the products of combustion, in natural gas and propane jet flames with crosswinds, and found Conversion Inefficiencies, (1-efficiency), to increase with u_c, and to decrease with increase in u. These changes are related

to changes in combustion modes, as is demonstrated by the dashed horizontal line at $U^* = 0.68$ in Fig. 2. Values of Re_c ranged between 1,083 and 26,905. Along it, are marked locations of three percentage values of conversion inefficiencies from [10]: 0.05% (u/u_c = 3), when rim-attached, and high inefficiencies of 0.56% and 11.3%, when downwash-attached. At the maximum Re_c downwash attachment had ceased, and only early downwash remained. The lowest inefficiency occurred at the lowest Re_c of 1,083, when the flame was rim-attached, with u=2.07 and u_c=0.7 m/s, u/u_c=0.3. Inefficiencies increased with increases in Re_c, and reduced with increases in U^*.

Downstream gases were monitored, in the present study, only for the presence of CH_4, using a Pulitong VI.18 methane gas detector. Only one location was found at which CH_4 was detected, 50 mm below the level of the burner exit plane, and 150 mm downstream of the centre of the burner pipe, with Re_c = 18,860, and $U^* = 0.3$. It is marked by an asterisk on line (*b*), just within the downwash-attached regime. Concentrations ranged between 562 and 683 ppm. Similarly, with natural gas flaring in the CanmetENERGY Flame Test Facility, no natural gas was found in the products [4].

8. Fire whirls

Fire whirls are created by high tangential circulations around a plentiful supply of fuel. They can be very powerful, generating devastating fire storms. Increasing circulation increases the burn rate, and reduces the plume radius. The relevant Critical Velocity group, *CV*, is based upon the critical wind velocity, U_c, at which the strongest fire whirl is generated, normalised by a gravitational velocity, $U_c/(gH)^{0.5}$ [13]. With g the acceleration of gravity, and H the length scale of the burning area, (D in Eq. (1)). This can be a pool diameter in a laboratory, a much larger, configuration of atmospheric burners, or a wildfire. The rotating chimney formed in this way creates a high velocity and low ground pressure.

A number of possible correlations were explored, and one, expressing CV as a function of U^*, was optimal. None could be expressed by the coordinates of Fig. 2. The length scale, H, appears in both groups and dominates the onset of fire whirl. Figure 6 shows values of CV that initiated whirls, as a function of U^*, and includes data derived from a variety of sources.

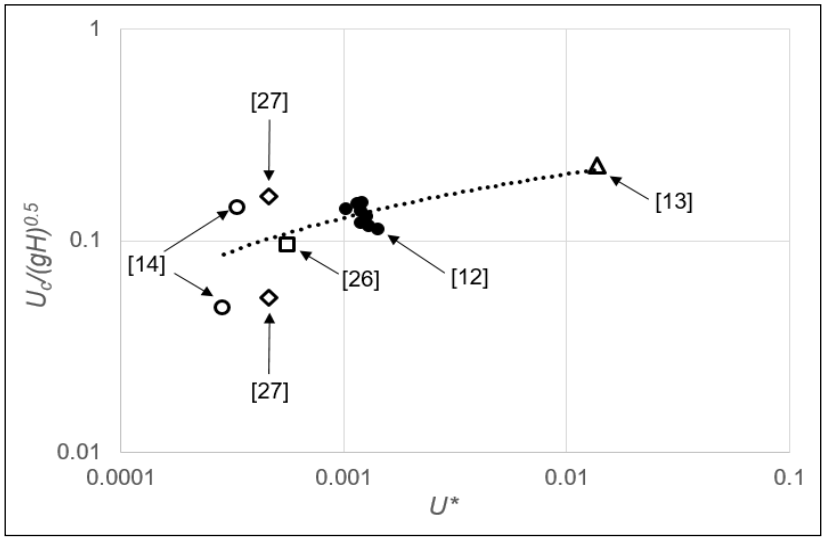

Fig. 6. Conditions for fire whirl initiation.

These include large atmospheric fires, ranging from the huge Hamburg warfare fire, covering about 11 km^2 [25], to the smaller scale laboratory studies in [12]. In these, the tangential air velocity, U_c, circulated around a central fuel pan, of diameter, H, up to 55 cm. With this, the power was 0.807 MW, and the whirl flame height 5.01 m. Following [14], the atmospheric experiments in [26], released 100 MW from 100 burners, over an area of 125 m x 125 m.

9. Conclusions

The paper examines the diverse basic regimes in which fuels can mix and react with air. Although by no means fully complete, it is a first attempt to provide a comprehensive overall generalisation of the different regimes and their boundaries. Major findings include:

(1). Save for fire whirls, regime boundaries of eight different jet flame types are identified in Fig. 2 in terms of plots of U^* against Re_c, supplemented by D/δ_k.

(2). The addition of cross flow air to lifted jet flames initially enhances the burning rate, but later inhibits it, as transitions can occur to rim attachment, downwash flames, and extinction.

(3). In downwash lifted jet flames with cross flow, no more than about a third of the total air required for combustion can be added to the fuel in this way.

(4). A core regime of downwash-attached jet flames is identified in Fig. 2, surrounded by one of rim-attached flames, bordering on downwash and blow-off regimes.

(5). The highest U^* values occur with lifted jet flames with cross flow. The most potentially energetic are capable of up to 600 MW.

(6). Fire whirls, which require correlating parameters, other than those in Fig. 2, have developed 100 MW experimentally. Coupled with firestorms, they are capable of warfare scale destruction.

(7). Few flame reaction localities were identified with significant unburned CH_4. Combustion inefficiencies increased with increased Re_c, and reduced with increased U^*.

References

[1] D. Bradley, P.H. Gaskell, Xiaojun Gu, The mathematical modeling of lift-off and blow-off of turbulent non-premixed methane jet flames at high strain rates, Proc. Combust. Inst. 27 (1998) 1199-1206.

[2] D. Bradley, P.H. Gaskell, Xiaojun Gu, A. Palacios, Jet flame heights, lift-off distances and mean flame surface density for extensive ranges of fuels and flow rates, Combust. Flame 164 (2016) 400-409.

[3] G. Chamberlain, Developments in design methods for predicting thermal radiation from flares, Chem. Eng. Res. Des. 65 (1987) 299-309.

[4] P. Gogolek, A. Caverly, R. Schwartz, J. Seebold, J. Pohl, Emissions from elevated flares – a survey of the literature. 2010, 88 pp, Canmet ENERGY, Ottawa.

[5] B.J. Lowesmith, G. Hankinson, Large scale high pressure jet fires involving natural gas and natural gas/hydrogen mixtures, Process Saf. Environ. 90 (2012) 108-120.

[6] G.T. Kalghatgi, Blow-out stability of gaseous jet diffusion flames part II: effect of cross wind, Combust. Sci. Tech. 26 (1981) 241-244.

[7] Qiang Wang, Longhua Hu, Sung Hwan Yoon, Shouxiang Lu, M. Delichatios, Suk Ho Chung, Blow-out limits of non-premixed turbulent jet flames in a cross flow at atmospheric and sub-atmospheric pressures, Combust. Flame 162 (2015) 3562-3568.

[8] R.F. Huang, J.M. Chang, The stability and visualized flame and flow structures of a combusting jet in cross flow, Combust. Flame 98 (1994) 267-278.

[9] F. Shang, L. Hu, X. Sun, Q. Wang, A. Palacios, Flame downwash length evolution of non-premixed gaseous fuel jets in cross-flow: experiments and a new correlation. Applied Energy. 198 (2017) 99-107.

[10] M.R. Johnson, L.W, Kostiuk, Efficiencies of low-momentum jet diffusion flames in crosswinds, Combust. Flame 123 (2000) 189-200.

[11] H.W. Emmons, S.-J. Ying, Fire Whirl, Proc. Combust. Inst. 11 (1967) 475-488.

[12] Kuibin Zhou, Naian Liu, Jesse S. Lozano, Yanlong Shan, Bin Yao, Kohyu Satoh, Effect of flow circulation on combustion dynamics of fire whirl, Proc. Combust. Inst. 34 (2013) 2617-2624.

[13] Kazunori Kuwana, Kozo Sekimoto, Kozo Saito, Forman A. Williams, Scaling fire whirls, Fire Safety Jour. 43 (2008) 252-257.

[14] J. Dessens, Man-made tornadoes, Nature, 4610 (1962) 13-14.

[15] T.F. Fric, A. Roshko,Vortical structure in the wake of transverse jet, J. Fluid Mech. 279 (1994),1-47.

[16] R.W. Grout, A Gruber, C. S. Yoo, J.H. Chen, Direct numerical simulation of flame stabilization downstream of a transverse fuel jet in cross flow, Proc. Combust. Inst. 33 (2011) 1629-1637.

[17] Göttgens, F. Mauss, N. Peters, Analytic approximations of burning velocities and flame thicknesses of lean hydrogen, methane, ethylene, ethane, acetylene and propane flames, Proc. Combust. Inst. 24 (1992) 129-135.

[18] D. Razus, D. Oancea V. Brinzea, M. Mitu, C. Movileanu, Experimental and computed burning velocities of propane–air mixtures, Energy Convers. Manage 51 (2010) 2979-2984.

[19] A. Vanmaaren, L.P.H. DeGoey, Stretch and the adiabatic burning velocity of methane- and propane-air flames, Combust. Sci. and Tech. 102(1994) 309-314.

[20] X. J. Gu , M.Z. Haq , M. Lawes , R. Wooley, Laminar burning velocity and markstein lengths of methane-air mixtures, Combust. Flame 121 (2000) 41-58.

[21] A. Palacios, D. Bradley, Generalised correlations of blow-off and flame quenching for sub-sonic and choked jet flames, Combust. Flame 185 (2017) 309-318.

[22] A. Palacios, D. Bradley D, Hydrogen generation, and its venting from nuclear reactors. Fire Safety Journal, (2020) doi.org10.1016j.firesaf.2020.102968.

[23] A.D. Johnson, H.M. Brightwell, A.J. Carsley, A model for predicting the thermal radiation hazards from large-scale horizontally released natural gas jet fires. Trans IChemE, 72(B) (1994) 157-166.

[24] G. Chamberlain, D. Bradley, P.H. Gaskell, Xiao-Jun Gu, D.R. Emerson, A computational study of turbulent non-premixed methane jet flames in a crosswind, Proc. 5th International Seminar on Fire and Explosion Hazards, Edinburgh UK, Eds. D. Bradley, D. Drysdale, V. Molkov, R. Carvel, University of Edinburgh, ISBN: 978-0-9557497-2-8, pp. 394-403 (2009).

[25] M.R. Johnson, L.W, Kostiuk, A parametric model for the efficiency of a flare in crosswind, Proc. Combust. Inst. 29 (2002) 1943-1950.

[26] C.H.V. Ebert, The meteorological factor in the Hamburg fire storm, Weatherwise, 16:2 (1963) 70-75.

[27] C.R. Church, J.T. Snow, J. Dessens, Intense atmospheric vortices associated with a 1000 MW fire, Bull, America Meteorological Soc. 61 (1980) 682-694.